WAVELET ANALYSIS OF WAVE PROPAGATION OVER POSIDONIA OCEANICA

PANAYOTIS PRINOS (1), THEOHARRIS KOFTIS (2) and PANAGIOTA GALIATSATOU (3)

(1) Professor, Department of Civil Engineering, Hydraulics Laboratory, Aristotle University of Thessaloniki, AUTh, Thessaloniki, 54124, Greece, prinosp@civil.auth.gr

(2) *Research Associate, Department of Civil Engineering, Hydraulics Laboratory, Aristotle University of Thessaloniki, AUTh, Thessaloniki, 54124, Greece, thkoftis@civil.auth.gr*

(3) *Research Associate, Department of Civil Engineering, Hydraulics Laboratory, Aristotle University of Thessaloniki, AUTh, Thessaloniki, 54124, Greece, pgaliats@civil.auth.gr*

In this work a wavelet analysis is performed for the experimental data of wave propagating over an artificial *Posidonia oceanica* meadow, obtained by large scale experiments that have been conducted in the CIEM wave flume. Main objective of this analysis is to measure the effects of plants submergence ratio h_s/D (h_s= height of seagrass, D= water depth) and seagrass density (stems/m^2) on the wave energy dissipation and on the wave induced velocities. Results show that the effect of seagrasses can be significant on the wave attenuation and that the dissipation of wave energy increases with the increase of the above mentioned seagrass parameters.

Keywords: Seagrasses; P. Oceanica; wavelet analysis; wave attenuation; wave-vegetation interaction.

1. Introduction

Seagrasses are marine flowering plants that have roots, stems and leaves and colonize. There are four European species of seagrasses: *Zostera marina*, *Zostera noltii*, *Cymodocea nodosa* and *Posidonia oceanica* (Borum et al., 2004), which is the most common seagrass species in the Mediterranean Sea and is usually distributed in shallow areas from the surface to a depth of 30-40 m in clear conditions. *P. Oceanica* can colonize soft substrates such as sand in wave-sheltered areas and also attach to rocks being exposed to relatively high wave energy and wind driven currents (Koch et al, 2006). The plant has ribbon-like leaves, 1.0 cm wide and up to 1.0 m long and the plants density varies from sparse (<150 stems/m^2) found in deeper waters to dense (>700 stems/m^2).

The importance of seagrasses regarding biological and physical aspects has been well recognized; due to their capacity to alter their environment, seagrasses have been referred to as "ecosystem engineers". Seagrass meadows are of great importance for maintaining biodiversity since they are highly productive and can serve as important nursery grounds for numerous species of algae, fish and invertebrates both above and below the seabed. Regarding the coastal protection aspect, a service commonly listed for seagrasses is sediment and shoreline stabilization, achieved by slowing water motion and current flow and by reducing sediment suspension, (Fonseca and Cahalan 1992; Borum et al 2004).

Regarding the hydrodynamics, a complex water flow system describes the situation, since not only water flow affects seagrasses (seagrass growth, increase of nutrient availability to the plants due to sedimentation), and seagrasses affect water flow (wave and current attenuation) but seagrasses and water flow may interact in highly coupled, nonlinear ways (Koch et al, 2006). The effects of seagrasses on unidirectional flows are well studied, while much less is known about the wave-seagrasses interaction. The degree of wave attenuation depends both on the seagrasses characteristics (the seagrass density, the canopy height, the stiffness of the plant and the bending of the shoots) and the wave parameters (wave height, period and direction) so the quantification of wave energy dissipation over seagrasses is difficult to expressed in a universal way (Mendez and Losada, 2004).

Numerical modelling for such wave-seagrasses interaction is a demanding task, since the parameters of the plant stiffness and movement with wave motion is difficult to model. Therefore in most theoretical and numerical studies the approximation of plants as rigid cylinders with different values to the drag coefficient is done (Dalrymple et al 1984, Kobayashi et al 1993, Agustin et al 2009, Li and Zhang, 2010). Various experimental studies on wave attenuation due to coastal vegetation have been performed, with large variability of the results for wave damping over seagrass meadows that confirm the complexity of such flow system. Ward et al. (1984) performed field measurements in a shallow estuarine embayment colonized by seagrass communities and showed that wave energy was attenuated by the vegetation, suppressing resuspension and enhancing deposition. In Fonseca and Cahalan (1992) a flume study was performed to measure wave reduction by the use of four species of seagrass. The results for wave attenuation were found in a wide range, from 20% to 76 % over 1 m length when the plants were occupying the entire water depth. Bouma et al. (2005) quantified the effect of stiffness of the plant since in their experimental study of the interaction of regular waves with seagrasses and artificial vegetation showed that dissipation was roughly three times higher in the case of vegetation with stiff leaves compared to that with flexible leaves. Recently in a flume study by Stratigaki et al (2010) the results for regular waves passing artificial *P. oceanica* meadows showed that damping of wave height depends on seagrass density and appears to be greater than 35% for a seagrass meadow having density of 360 stems/m^2 and occupying half the water column.

In this work large scale experiments have been conducted in the CIEM (Canal d'Investigació i Experimentació Marítima) wave flume for the measurement of wave height propagation over artificial *P. oceanica* meadow in intermediate waters. The focus of this study is to measure the effects of plants submergence ratio h_s/D (h_s= height of seagrass, D= water depth) and seagrass density (stems/m^2) on the wave energy dissipation and on the wave induced velocities. For irregular waves, three different submergence ratios (h_s/D equal to 0.50, 0.42 and 0.37) and two seagrass densities (360 and 180 stems/m^2) are tested while measurements of wave elevation and wave induced velocities are taken at several locations along the *P. oceanica* meadow. A wavelet analysis is performed for the above mentioned time series for the identification of the main frequencies present in the data, as well as the time intervals they appear in and to determine the dominant non-stationarities of the signals.

2. Experimental setup

The CIEM wave flume is 100m long, 5m deep and 3 m wide. A sandy slope beach of 1:15 was installed at the end of the flume for the elimination of wave reflection. A 20 m long horizontal and flat sandy area was created in the central part of the flume and the patch of artificial *P. oceanica*, with a total length L=10.70 m and height h_s=0.55m, was placed above, as shown in Fig. 1. The seagrass mimics were made of polypropylene strips and carefully designed to reproduce the flexibility and buoyancy properties typical of the natural *P. oceanica* plants. Fig. 2 shows the dimensions and structure of the mimics, while full details on the mimics and on the experiment setup can be found in Stratigraki et al (2010).

The tests were performed for irregular intermediate water waves (kD =0.76-0.92) for three different submergence ratios h_s/D (0.37, 0.42 and 0.50) and two different plant densities (360 and 180 stems/m^2) as shown in Table 1. The densities chosen are representatives of shallow sparse *P. oceanica* patches found in nature. Wave transformation was monitored by wave gauges distributed along the flume. Velocities were measured at 3 locations (0.70m in front of the meadow, 1.80m and 8.00m within the meadow, or made dimensionless with the meadow length L, at x/L=-0.07, 0.17 and 0.80 respectively) at 4 different elevations from the flume bed (at z=0.20m, 0.40m, 0.60m and 0.80m or made dimensionless with seagrasses height h_s, at z/h_s=0.36, 0.72, 1.09 and 1.45 respectively). The location of the wave gauges and current meters along the meadow is shown in Fig. 3.
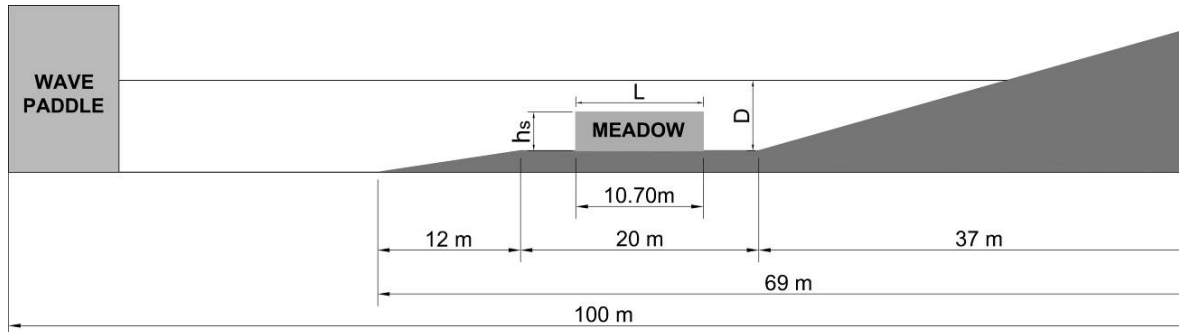

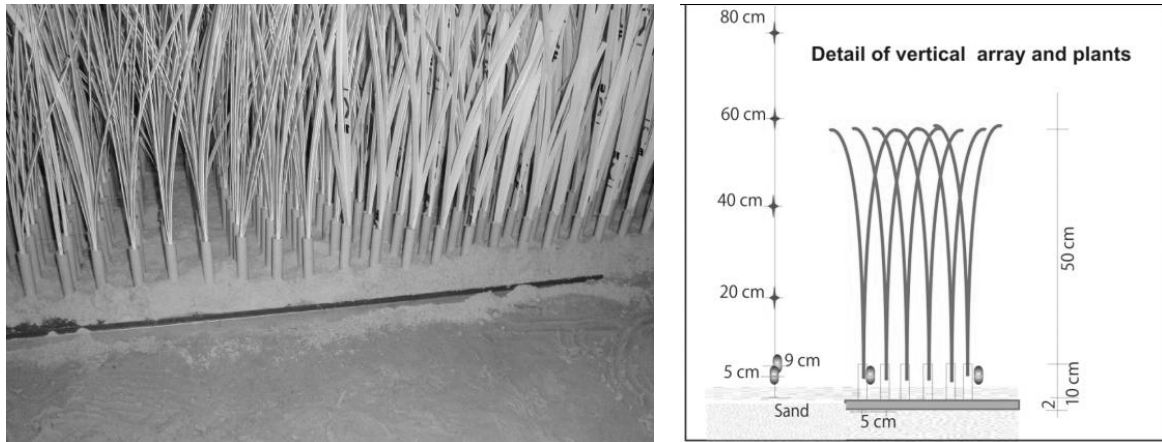Figure 1. Sketch of the experimental setup of the CIEM flume

Figure 2. Detail and schematic detail of the artificial plants

Table 1 Wave and plant characteristics.

Water depth at meadow D (m)	Seagrasses height h_s (m)	Wave height H_s (m)	Peak period T_p (s)	kD	Plant density (stems/m^2)	Submergence ratio h_s/D
1.50	0.55	0.40	3.0	0.92	360	0.37
1.30	0.55	0.40	3.0	0.84	360	0.42
1.10	0.55	0.40	3.0	0.76	360	0.50
1.10	0.55	0.40	3.0	0.76	180	0.50

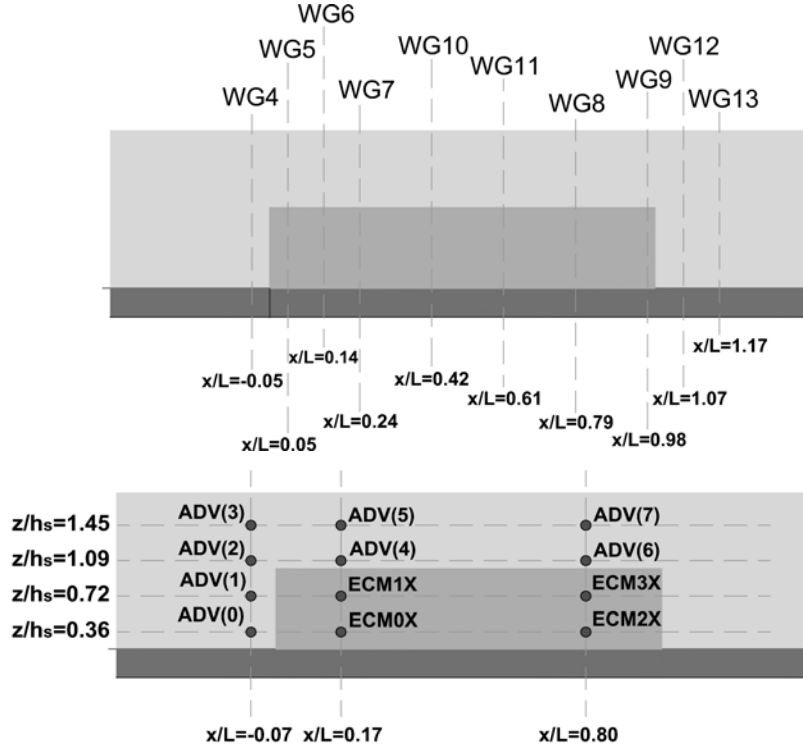Figure 3. Location of resistive wave gauges and current-meters across meadow

3. Wavelet Analysis

Wavelet analysis is a modern technique in signal processing, which has evolved in the recent years and is most commonly used in the analysis of non-stationary signals. It should also be noted that real-world signals often have frequencies that can change over time or have anomalies, or other "events" at certain specific times. The inability of the Fourier transform to accurately represent signals that have such non-periodic components that are localised in time or space is in favor of the wavelet transform. This is due to the Fourier transform being based on the assumption that the signal to be transformed is periodic in nature and of infinite length. Wavelet transforms do not have a single set of basis functions like the Fourier transform, which utilizes just the sine and cosine functions. Instead, wavelet transforms have an infinite set of possible basis functions. Thus wavelet analysis provides immediate access to information that can be obscured by other time-frequency methods such as Fourier analysis. Another deficiency of the Fourier transform is its inability to provide any information about the time dependence of a signal, as results are averaged over the entire duration of the signal. This is a problem when analysing signals of a non-stationary nature, where it is often beneficial to be able to acquire a correlation between the time and frequency domains of a signal.

The wavelet transform breaks the signal into wavelets, which are scaled and shifted versions of the mother (parent) wavelet ψ_0. In the case of wavelets, time-frequency representations are normally replaced by time-scale representations. The continuous wavelet transform of a discrete sequence x_n is defined as the convolution of x_n with a scaled and translated version of the mother (parent) wavelet (Kijewski-Correa and Kareem, 2007). The wavelet

coefficients provide a measure of the similarity between the dilated/ shifted parent wavelet and the signal at time t and scale s. One of the most extensively used mother wavelets is the Morlet wavelet:

$$\psi_0(\eta) = \pi^{-1/4} e^{i\omega_0\eta} e^{-\eta^2/2} \qquad [1]$$

where η is a nondimensional time parameter and ω_0 is the nondimensional frequency. According to Farge (1992), for the Morlet wavelet to satisfy the admissibility condition (Kaiser, 1994), this frequency should be equal to 6. The Morlet wavelet is a common nonorthogonal complex wavelet. For the Morlet wavelet, the scale s and the Fourier period are nearly identical.

In the present work, the wavelet coefficients $W_n(s)$ are calculated using the convolution theorem and spectral representation of the wavelet transform (Farge, 1992):

$$W_n(s) = \sum_{k=0}^{N-1} \hat{x}_k \hat{\psi}^*(s\omega_k) \; e^{i\omega_k n\delta_t} \qquad [2]$$

where ω_k is the angular frequency, ψ^* is the complex conjugate of the wavelet ψ, the variable s is the scale of the wavelet transform, δ_t is the equal time spacing of the observations of x_n, $n=0,1,\dots N\text{-}1$ is the localized time index of the time series and N is the number of points in the time series.

The squared magnitude of the wavelet coefficients $|W_n(s)|^2$ can be presented as energy content in frequency and time and is called wavelet power spectrum. The wavelet power spectrum describes the variance of the time series at a selected scale (period) and at a selected moment in time (Torrence and Webster, 1998). To compare different wavelet power spectra, a normalization is performed, dividing the wavelet power spectrum by the variance of a white-noise time series σ^2_{wn} ($|W_n(s)|^2 / \sigma^2_{wn}$) giving a measure of the power relative to white noise.

The scale-averaged wavelet power spectrum is used to examine fluctuations in power over a range of scales. It is obtained by averaging the local wavelet coefficients along the N-vertical cuts of the time axis for a range of scales from s_1 to s_2 (Markovic and Koch, 2005):

$$\overline{W_n}^2 = \frac{\delta_j \delta_t}{C_\delta} \sum_{j=j_1}^{j=j_2} \frac{|W_n(s_j)|^2}{s_j} \qquad [3]$$

where δ_j depends on the width in spectral-space of the wavelet function, while C_δ is a constant for each wavelet function. Compared to the most commonly used Fourier transform which does not give any information of the signal in the time domain, the wavelet transform is localized in both time and frequency domains. Therefore the construction of the scale-averaged wavelet power spectrum, which detects statistically significant periodicities along the whole time series, cannot be created for the simple Fourier transform.

The average of the wavelet power over all local wavelet spectra along the time axis is the global wavelet power spectrum (Torrence and Compo, 1998):

$$\overline{W}^2(s) = \frac{1}{N} \sum_{n=0}^{N-1} |W_n(s)|^2 \qquad [4]$$

Percival (1995) has shown that the global wavelet power spectrum provides an unbiased and consistent estimation of the true power spectrum of a time series. Kestin et al., (1998) suggest that the global wavelet spectrum can provide a useful measure of the background spectrum, against which peaks in the local wavelet spectra could be tested.

4. Analysis of results

The analysis performed in this study is shown in Fig. 4, where the measured water surface elevation at WG5, just after seaward the plant meadow edge (x/L=0.05) is processed for the meadow with submergence ratio $h_s/D= 0.50$ and density 360 stems/m^2. The wavelet power spectrum is shown in Fig. 4(b) for the time series of water surface elevation found in Fig. 4(a). We can identify the main frequencies found in the data in the range of 2-4s, over all the measured time history of about 800s. This is more obvious in the global wavelet spectrum plot in Fig. 4(c), with the peak period of 3s of the incident water wave shown. A smaller second peak for low frequency components of the wave is observed in this graph which is not found in the spectrum of the water elevation in the beginning of the flume, WG0, as shown in Fig. 4(d). This might be due to the nonlinear interactions of the plant leaves with the water motion resulting in transferring energy from the high to the smaller frequency components of the wave spectrum.
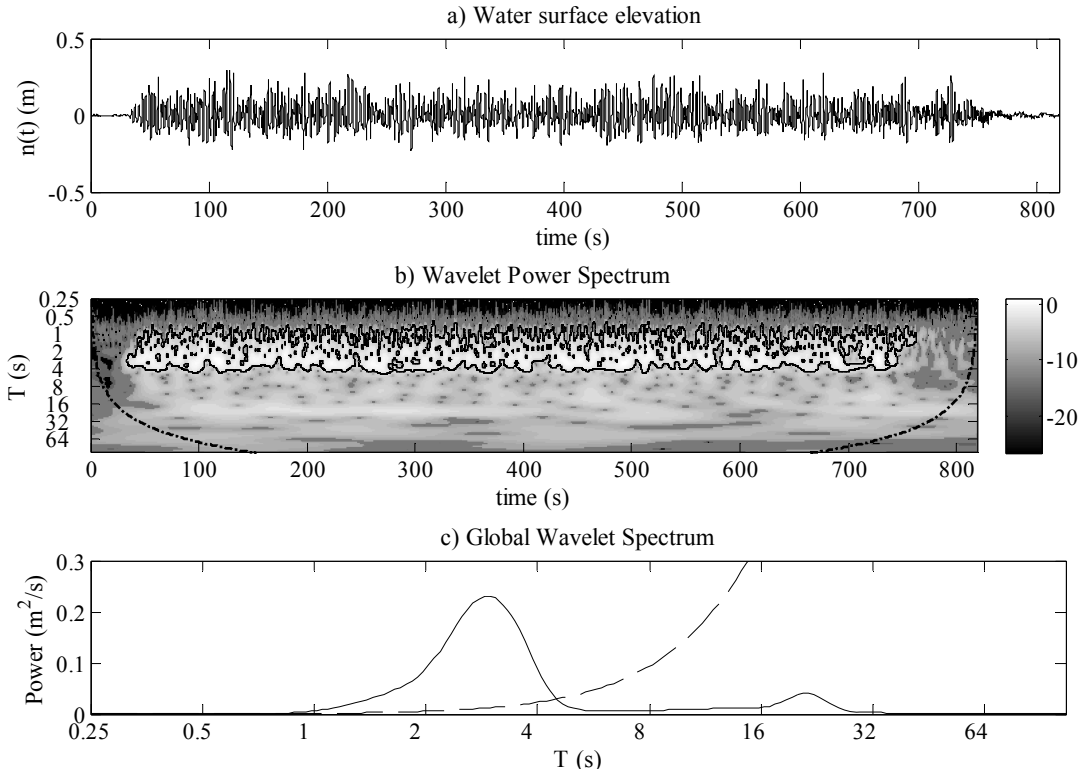
a) Water surface elevation

b) Wavelet Power Spectrum

c) Global Wavelet Spectrum

Figure 4. (a) Time series of water surface elevation, (b) wavelet power spectrum and (c) global wavelet spectrum, at WG5 (x/L=0.05) (h_s/D=0.50 and 360 stems/m^2)
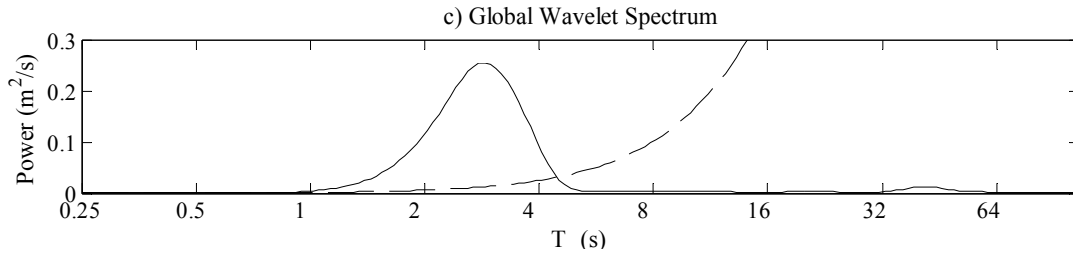
c) Global Wavelet Spectrum

Figure 4. (d) Global wavelet spectrum at beginning of wave flume, at WG0 (x/L=-2.20) (h_s/D=0.50 and 360 stems/m^2)

The effect of the seagrasses on the wave propagation over the meadow and the resultant energy dissipation can be seen in Fig. 5, where the wave energy spectrum measured in the wave gauges is depicted for all the examined plant configurations. There is a gradual decrease of the wave energy along the meadow due to the friction inserted in the flow by the seagrass meadow. Wave energy dissipation is obvious for all components of the wave spectra, especially at peak frequencies.

Comparing the results for the plant with density of 360 stems/m^2 and the three different submergence ratios of h_s/D= 0.37, 0.42 and 0.50 shown in Fig. 5, we can identify the significance of this parameter in wave attenuation by vegetation. For the higher meadow (h_s/D= 0.50) the maximum value of the global wavelet spectrum is reduced about 55% (from 0.23m^2/s at x/L=-0.05 to 0.10 m^2/s at x/L=0.98), while for the lower meadow (h_s/D= 0.37) the maximum value of the global wavelet spectrum is reduced about 32%. Regarding the effect of plant density, this can be seen by comparing Fig. 5(a) and 5(d), where the global wave spectrum for the dense (360 stems/m^2) and the sparse (180 stems/m^2) for h_s/D= 0.50, is shown. The maximum value of the global wavelet spectrum is reduced by 37% for the sparse meadow, much less compared to the 55% decrease for the dense meadow.

It can also be noticed that due to the "plant resistance" to the flow, in the seaward side of the meadow, part of the wave energy is reflected and the wave height increases in the edge of the meadow (x/L=0.05) for the more dense case (360 stems/m^2). Also when exiting the meadow (x/L=1.17) the flow is "reconstructed", with the energy transfer back to the main wave frequency components, resulting in a small increase in the wave energy of the peak period.
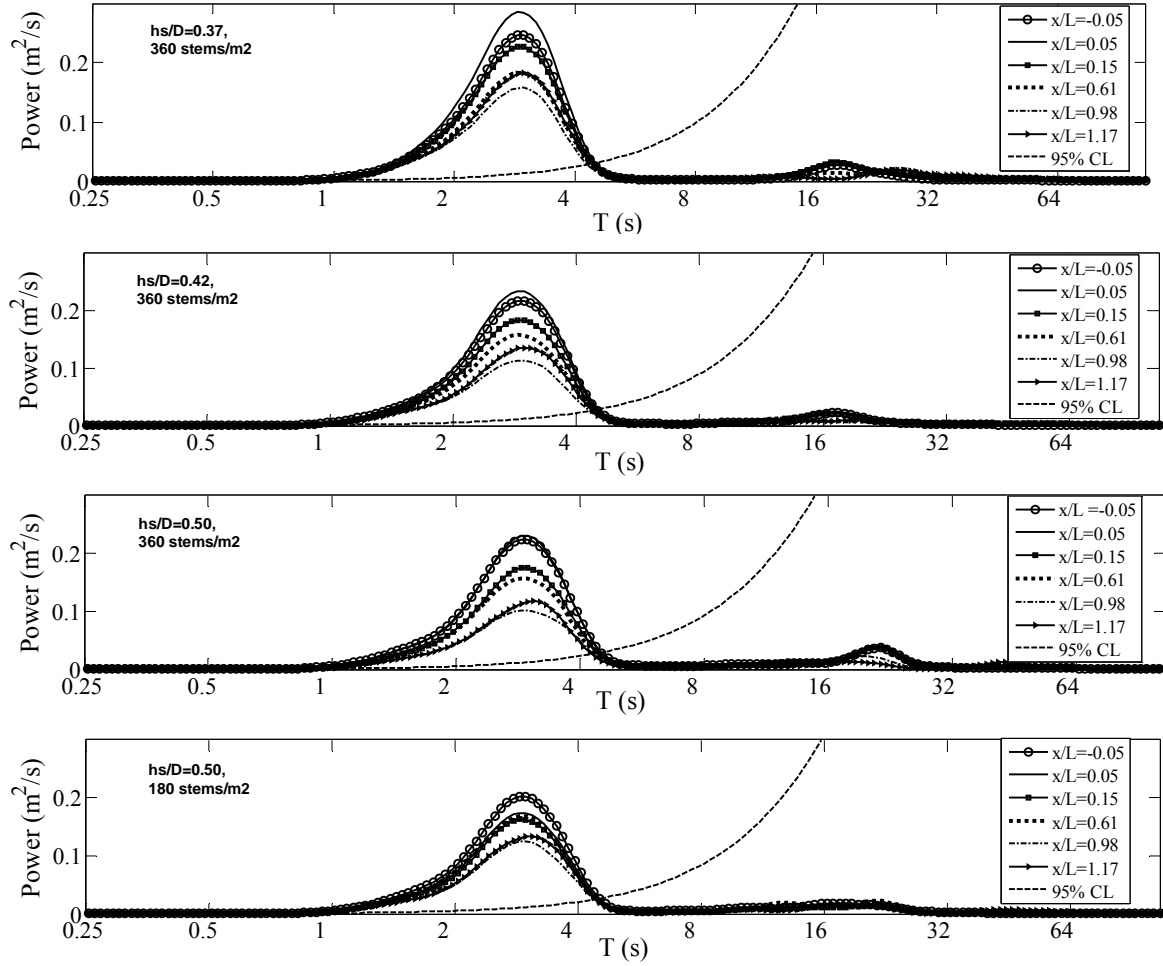
Figure 5. Wave spectra along the meadow for plant characteristics (a) $h_s/D=0.37$, 360 stems/m^2 (b) $h_s/D=0.42$, 360 stems/m^2, (c) $h_s/D=0.50$, 360 stems/m^2, (d) $h_s/D=0.50$, 180 stems/m^2

The analysis is extended for the investigation of the effect of the *P. oceanica* meadow parameters on the velocities measured at the current meters shown in Fig. 3. Fig. 6(a), shows the time series of the horizontal velocity at ADV0 located in front of the meadow ($x/L=-0.07$) and in the lowest vertical position ($z/h_s=0.36$), Fig. 6(b) the wavelet power spectrum and Fig. 6(c) the global wavelet spectrum for the meadow with submergence ratio $h_s/D=0.50$ and density 360 stems/m^2. For this experiment ($h_s/D=0.50$ and 360 stems/m^2) the velocity spectrum at the three positions measured ($x/L=-0.07$, 0.17 and 0.80) and the four vertical positions ($z/h_s=0.36$, 0.72, 1.09 and 1.45) is shown in Fig. 7. It can be seen that for the highest above meadow position ($z/h_s=0.36$) and in the lowest inside meadow position ($z/h_s=0.36$) the velocities are decreased significantly for all wave components, and the maximum value of the spectrum for the peak period is reduced by 33% (from 2.17 m^{2}s^{-3} to 1.44 m^{2}s^{-3}) and 85% (from 1.70 m^{2}s^{-3} to 0.27 m^{2}s^{-3}) respectively. For the velocities just below and above the meadow edge, $z/h_s=0.72$ and 1.09 respectively, the decrease is much smaller due to the nonlinear interactions and the 3D effects inserted in the flow by the plant leaves. The second peak at low frequency components of the wave is more obvious in this plot inside the meadow ($x/L=0.17$ and 0.80) compared to that observed in the spectrum of the water elevation.

The effect of the submergence of the meadow on the velocities can be seen by comparing the velocity spectrum for the plant with density of 360 stems/m^2 and submergence ratios of $h_s/D=0.37$ and 0.50, as shown in Fig. 8. For the lowest in meadow position shown in Fig. 8(a) ($z/h_s=0.36$) the reduction for the maximum value of the velocity spectrum is significant for both the highest meadow (85% for $h_s/D=0.50$) and the lowest meadow (80% for $h_s/D=0.37$). As mentioned above, this reduction is less obvious for $z/h_s=0.72$ and 1.09, as seen from Fig. 8(b) and (c). The effect of plant's density on the velocities can be seen by comparing the velocity spectrum for submergence ratio of $h_s/D=0.50$ and the sparse (180 stems/m^2) and the dense (360 stems/m^2) meadow, as shown in Fig.9. The differences for the velocity energy spectrum attenuation for the two plant densities are not significant, with the greater attenuation of the wave induced velocities occurring for the dense plant.
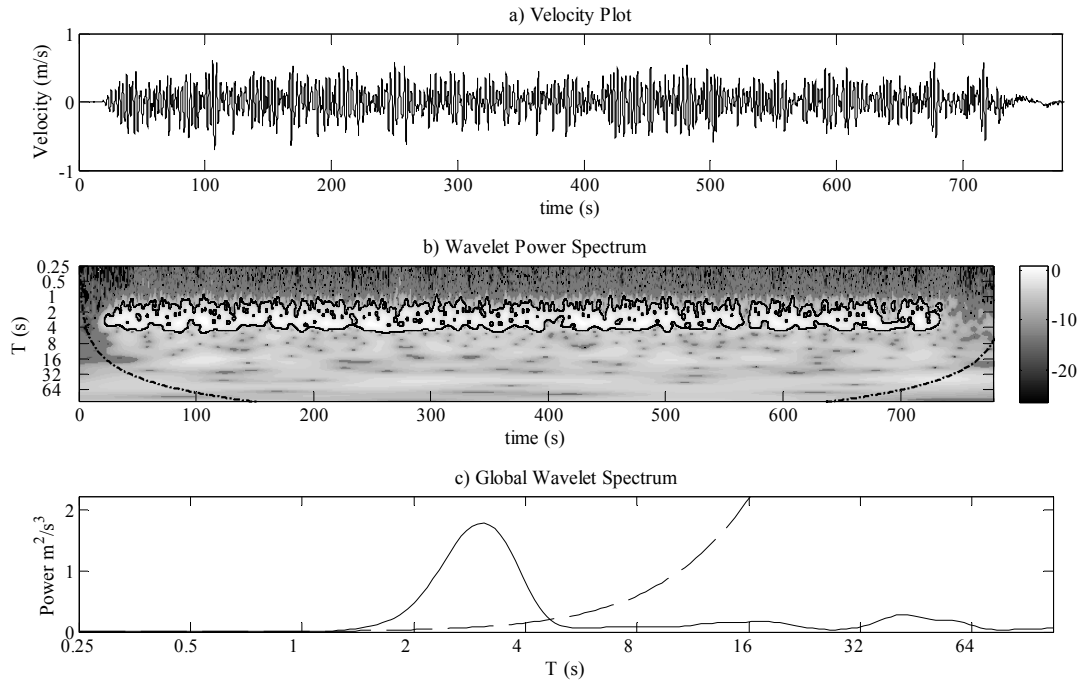
a) Velocity Plot

b) Wavelet Power Spectrum

c) Global Wavelet Spectrum

Figure 6. (a) Time series of measured velocity, (b) wavelet power spectrum and (c) global wavelet spectrum, at ADVO (x/L=-0.07, z/h$_s$=0.36) (h$_s$/D=0.50 and 360 stems/m^2)
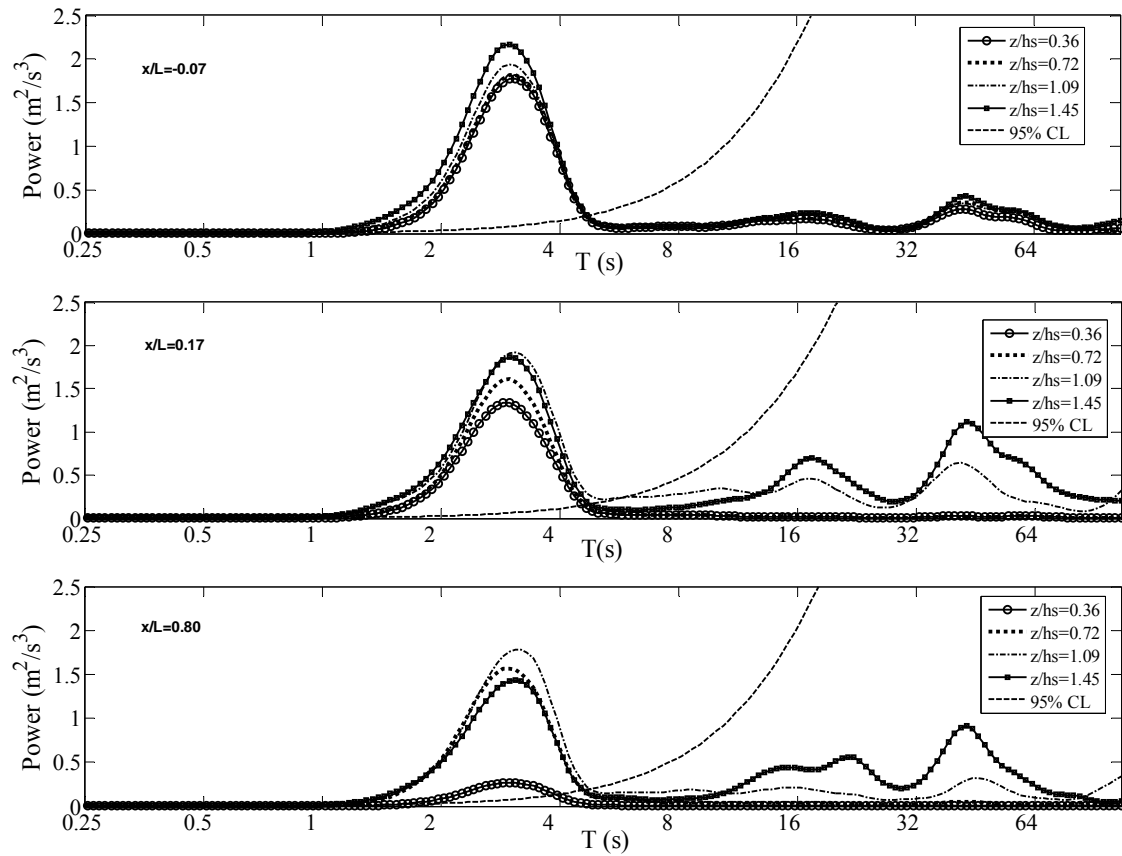

Figure 7. Velocity spectrum for h$_s$/D=0.50 and 360 stems/m^2 at (a) x/L=-0.07, (b) x/L=0.17, (c) x/L=0.80

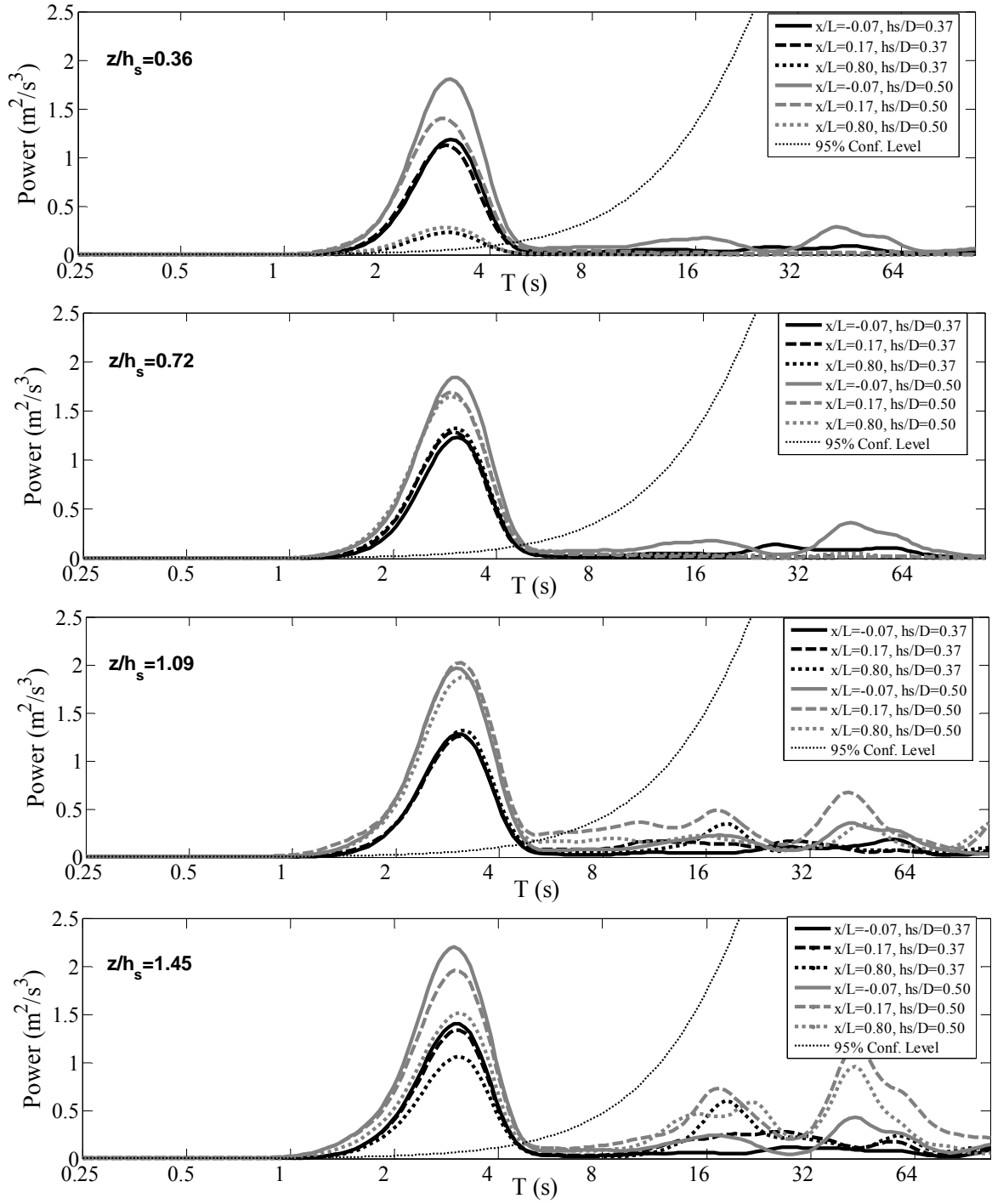Figure 8. Velocity spectrum for 360 stems/m^2 and h$_s$/D=0.37 and h$_s$/D=0.50, at (a) z/h$_s$=0.36, (b) z/h$_s$=0.72, (c) z/h$_s$=1.08, (d) z/h$_s$=1.45
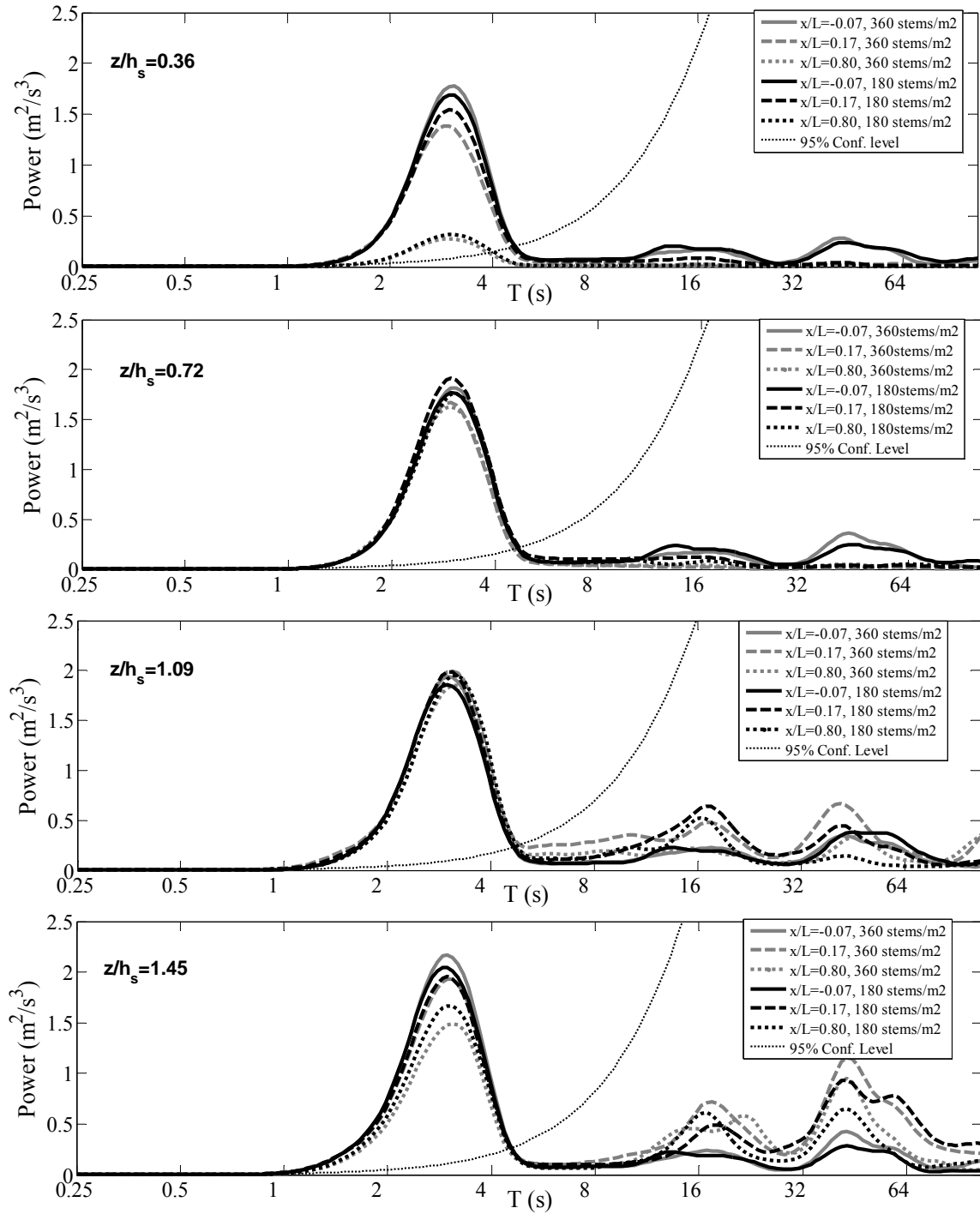
Figure 9. Velocity spectrum for $h_s/D=0.50$ and 180 stems/m^2 and 360 stems/m^2, at (a) $z/h_s=0.36$, (b) $z/h_s=0.72$, (c) $z/h_s=1.08$, (d) $z/h_s=1.45$

5. Conclusions

In this study, a wavelet analysis of experimental data of wave propagation over *P. Oceanica* meadow has been performed. The main conclusions can be summarized to the following:

- The effect of seagrasses can be significant on the wave attenuation. The maximum value of the power spectrum of the water elevation is reduced as wave propagates over meadow; maximum reduction ~55% at the end of meadow (x/L=0.98) occurs for the meadow with submergence ratio h_s/D=0.50 and density 360 stems/m^2.
- The wave energy attenuation depends on the submergence ratio of the meadow and the plant's density, and increases with the increase of these two parameters.
- Significant reduction of the wave induced velocities occurs at the lower part of the canopy (z/h_s=0.36) for all configurations, with maximum reduction on the maximum value of the velocity spectrum ~ 85% found for the meadow with submergence ratio h_s/D=0.50 and density 360 stems/m^2. Complex velocity field is observed near the edge of the meadow (z/h_s=0.72 and z/h_s=1.09).

References

Augustin L.N., Irish J.L. and Lynett P. (2009). 'Laboratory and numerical studies of wave damping by emergent and near emergent wetland vegetation', Coastal Engineering, Vol. 56, Issue 3, pp. 332-340.

Borum J., Duarte C.M., Krause-Jensen D. Greve T.M. (2004). 'European seagrasses: an introduction to monitoring and management'. Monitoring and Managing of European Seagrasses Project.

Bouma T.J., De Vries M.B., Low E., Peralta G., Tanczos J.C., Van De Koppel J., Herman P.M.J. (2005). 'Trade-offs related to ecosystem engineering: A case study on stiffness of emerging macrophytes', Ecology, Vol. 86, Issue 8, pp. 2187-2199.

Dalrymple R.A., Kirby J.T. and Hwang P.A. (1984). 'Wave Diffraction Due to Areas of Energy Dissipation', Journal of Waterway, Port, Coastal, and Ocean Engineering, Vol. 110, Issue 1, pp. 67-79.

Farge M (1992). 'Wavelet transforms and their applications to turbulence', Ann. Rev. Fluid Mech., 24, pp. 395-457, doi:10.1146/annurev.fl.24.010192.002143.

Fonseca M.S., Cahalan J.H. (1992). 'A preliminary evaluation of wave attenuation by four species of Seagrass', Estuarine, Coastal and Shelf Science, 35 (6), pp. 565-576.

Kaiser G (1994). 'A friendly guide to wavelets', Birkhauser, Boston.

Kestin T A, Karoly D J, Yano J I, Rayner N (1998) 'Time- frequency variability of ENSO and stochastic simulations', J. Climate 11(9), pp. 2258-2272, doi: 10.1175/1520-0442(1998)011<2258:TFVOEA>2.0.CO;2.

Kijewski-Correa T, Kareem A (2007) 'Performance of wavelet transform and empirical mode decomposition in extracting signals embedded in noise', J. Eng. Mech. – ASCE, 133(7), pp. 849-852.

Kobayashi N., Raichlen A.W., Asano T. (1993). 'Wave Attenuation by Vegetation', Journal of Waterway, Port, Coastal, and Ocean Engineering, Vol. 119, Issue 1, pp. 30-48.

Koch E.W., Sanford L.P., Chen S-N., Shafer D.J., Mckee Smith J. (2006). 'Waves in seagrass systems: Review and Technical recommendations', US Army Corps of Engineers®. Technical Report, ERDC TR-06-15.

Markovic D, Koch M (2005). 'Wavelet and scaling analysis of monthly precipitation extremes in Germany in the 20th century: Interannual to interdecadal oscillations and the North Atlantic Oscillation influence', Water Resour. Res. 41. W09420. doi: 10.1029/2004WR003843

Li C.W. and Zhang M.L. (2010). '3D modelling of hydrodynamics and mixing in a vegetation field under waves', Computers & Fluids, Vol. 39, Issue 4, pp. 604-614.

Mendez F.J. and Losada I.J. (2004). 'An empirical model to estimate the propagation of random breaking and nonbreaking waves over vegetation fields', Coastal Engineering, Vol. 51, Issue 2, pp. 103-118.

Percival DP (1995). 'On estimation of the wavelet variance', Biometrika 82(3): 619-631

Stratigaki V., Manca E., Prinos P., Losada I., Lara J., Sclavo M., Caceres I. , Sanchez-Arcilla A. (2010). 'Large scale experiments on wave propagation over Posidonia oceanica', Journal of Hydraulic Research, IAHR (accepted for publication).

Torrence Ch, Compo GP (1998). 'A practical guide to wavelet analysis', B. Am. Meteorol Soc. (BAMS), 79(1), pp. 61-78.

Torrence C, Webster P (1999). 'Interdecadal changes in the ENSO-Monsoon System', J. Climate 12(8), pp. 2679-2690. doi : 10.1175/1520-0442(1999)012<2679:ICITEM>2.0.CO;2

Ward L.G., Kemp W.M., and Boynton W.E. (1984). 'The influence of waves and seagrass communities on suspended particulates in an estuarine embayment', Marine Geology, Vol. 59, pp. 85-103.